

# Extraction of neutron structure from tagged structure functions

W. Cosyn<sup>\*,†</sup> and M. Sargsian<sup>\*</sup>

<sup>\*</sup>*Department of Physics, Florida International University, Miami, Florida 33199, USA*

<sup>†</sup>*On leave from: Department of Physics and Astronomy, Ghent University, Proeftuinstraat 86, B-9000 Gent, Belgium*

**Abstract.** We present work in a model used to describe semi-inclusive deep inelastic scattering off the deuteron. The model uses the virtual nucleon approximation to describe the interaction of the photon with the bound neutron and the generalized eikonal approximation is applied to calculate the final-state interaction diagram. Comparison with data taken at Jefferson Lab shows good agreement in the covered range of kinematics and points at a largely suppressed off-shell rescattering amplitude. The  $W$  and  $Q^2$  dependences of the total cross section and slope factor of the interaction of DIS products,  $X$ , off the spectator nucleon are extracted. Starting from the JLab data and our model calculations, we outline and apply an extrapolation method to obtain the neutron structure function  $F_{2N}$  at high Bjorken  $x$ .

**Keywords:** deep-inelastic scattering, final-state interaction, neutron structure function

**PACS:** 11.80.-m, 13.60.-r, 13.85.Ni

## INTRODUCTION

A reaction that can be used to study the influence of QCD dynamics at nucleonic length scales is semi-inclusive deep inelastic scattering off the deuteron ( $d(e, e' p_s)X$ ), where a spectator proton is detected in the final state. At very low spectator momenta the neutron is nearly on-shell and the reaction can be used to extract information about the “free” neutron structure function in a way that minimizes the nuclear binding effects inherent in scattering off a deuteron target. At higher spectator momenta the reaction can be used to study the modifications of nucleon properties and the role quark degrees of freedom in high density configurations of the deuteron. In kinematics which favour final-state interactions (FSI), the space-time evolution of hadronization can be examined. Two recent Jefferson Lab Hall B experiments have studied the reaction: one at high [1], and the other at low spectator momenta [2].

In order to provide meaningful interpretations of the measured data, theoretical models that quantify the importance of the FSI in the reaction are needed. The major difficulty in doing this is that one lacks detailed information about the composition and space-time evolution of the hadronic system produced in the deep inelastic scattering and how this changes as a function of Bjorken  $x$  and  $Q^2$ . Several theoretical approaches that provide models for the  $d(e, e' p_s)X$  reaction can be found in the literature [3, 4, 5, 6, 7, 8, 9, 10]. In the following, we will present work in a model based on the general properties of soft rescattering [11]. Results are compared to data taken in the JLab Deeps experiment and we use these results and data to describe a method to extract the neutron structure at high  $x$ .

## FORMALISM

The interaction of the virtual photon with the bound nucleon is treated with the *virtual nucleon approximation* (VNA) [4, 5, 12]. In the VNA, the spectator nucleon is taken on the mass shell, while the virtual photon interacts with an off-shell nucleon. The VNA is based on the following main assumptions: (i) only the  $pn$  component of the deuteron wave function is considered in the reaction, (ii) the negative energy projection of the virtual nucleon propagator gives negligible contribution to the scattering amplitude, and (iii) interactions of the virtual photon with exchanged mesons is neglected. Assumptions (i) and (ii) can be satisfied when the momentum of the spectator proton is limited to  $p_s \leq 700$  MeV/c [13], while (iii) is satisfied at large  $Q^2$  ( $> 1$  GeV<sup>2</sup>) [14, 15].

The nuclear wave function in the VNA is normalized to account for the baryon number conservation [16, 17, 18, 19]:

$$\int \alpha |\Psi_D(p)|^2 d^3 p = 1, \quad (1)$$

where  $\alpha = 2 - \frac{2(E_s - p_{s,z})}{M_D}$  is the light cone momentum fraction of the deuteron carried by the bound nucleon normalized in such a way that the half of the deuteron momentum fraction corresponds to  $\alpha = 1$ . Because of the virtuality of interacting nucleon it is impossible to satisfy the momentum sum rule at the same time, which can be qualitatively interpreted as part of the deuteron momentum fraction being distributed to non-nucleonic degrees of freedom.

In the model, two Feynman diagrams are taken into account: the plane-wave diagram where the on-shell proton is a pure spectator and the FSI diagram where a soft rescattering occurs between the produced  $X$  and the spectator. To describe the FSI of the produced  $X$  with the spectator nucleon, the *generalized eikonal approximation* is applied. At the energies under consideration in the JLab experiments, we can assume the rescattering to be diffractive and occurring over small angles. The following eikonal form is adopted for the  $X - N$  rescattering amplitude:

$$f_{X'N, XN} = \sigma(Q^2, x_{Bj})(i + \varepsilon(Q^2, x_{Bj}))e^{\frac{B(Q^2, x_{Bj})}{2}t}, \quad (2)$$

where  $\sigma$ ,  $\varepsilon$  and  $B$  are the effective total cross section, real part and the slope factor of the diffractive  $X'N \rightarrow XN$  scattering amplitude. In the derivation of the FSI amplitude, a factorized approach is used, whereby the interaction of the virtual photon with the off-shell nucleon is taken out of the integration over the intermediate spectator momentum. Such an approximation is also applied in quasi-elastic scattering [20, 13], being valid up to spectator momenta around 400 MeV/c.

We define the lab frame four-momenta of the involved particles as  $p_D \equiv (M_D, 0)$  for the deuteron,  $q \equiv (\nu, \vec{q})$  for the virtual photon (with the z-axis chosen along  $\vec{q}$ ),  $p_s \equiv (E_s = \sqrt{\vec{p}_s^2 + m_p^2}, \vec{p}_s)$  for the spectator proton and  $p_x \equiv (E_X, \vec{p}_X) = (\nu + M_D - E_s, \vec{q} - \vec{p}_s)$  the center of mass momentum of the undetected produced hadronic system  $X$ . The initial momentum of the bound off-shell neutron is defined as  $p_i \equiv p_D - p_s$ . After applying all the abovementioned approximations and averaging over  $\phi$  (the angle between the

electron and  $\gamma^*$ ,  $\vec{p}_s$  plane), we can write for the differential cross section [11]:

$$\frac{d\sigma}{d\hat{x}dQ^2d^3p_s} = \frac{4\pi\alpha_{EM}}{Q^2\hat{x}} \frac{|q|}{m_n} \left(1 - y - \frac{x^2y^2m_n^2}{Q^2}\right) \left(\frac{Q^2}{|q|^2} + \frac{2\tan^2\frac{\theta_e}{2}}{1+R}\right) \left|\frac{\alpha_i}{\alpha_q} + \frac{1}{2\hat{x}}\right|^{-1} \\ \times \left[\left(\frac{\alpha_i}{\alpha_q} + \frac{1}{2\hat{x}}\right)^2 + \frac{p_T^2}{2Q^2}\right] F_{2N}(\alpha_i, \hat{x}, Q^2) S^D(p_s). \quad (3)$$

$\alpha_{EM}$  is the fine-structure constant,  $-Q^2 = v^2 - \vec{q}^2$  is the four-momentum transfer,  $m_n$  the neutron mass,  $y = \frac{v}{E_e}$ ,  $\alpha_i = \frac{2p_i^-}{M_D}$ ,  $\alpha_q = \frac{2q^-}{M_D}$ ,  $\hat{x} = \frac{Q^2}{2p_i \cdot q}$  is the Bjorken  $x$  for a moving nucleon,  $\theta_e$  is the electron scattering angle,  $R = \frac{\sigma_L}{\sigma_T} \approx 0.18$  is the ratio of the longitudinal to transverse cross section for scattering off the nucleon, and  $F_{2N}$  is the effective nucleon structure function, which is defined at  $\hat{x}$  and in principle could be modified due to the nuclear binding (see e.g. Ref. [4]). We use the SLAC parametrization of Ref. [21] for  $F_{2N}$ .

In Eq. (3), the distorted spectral function  $S^D(p_s)$  contains the contributions from the plane-wave and FSI diagram and takes the following form:

$$S^D(p_s) = \frac{1}{3} \sum_{S_D, S_s, S_i} \left| \Psi^{SD}(p_i S_i, p_s S_s) + \frac{i}{2} \int \frac{d^2 p_{s', \perp}}{(2\pi)^2} \frac{\beta(s, m_{X'})}{4 |\vec{q}| \sqrt{E_s E_{s'}}} \right. \\ \left. \times \left[ \langle X, p_s | f_{X'N, XN}^{\text{on}}(s, t) | X', p_{s'} \rangle \Psi^{SD}(\vec{p}_{s'}, S_i, S_s) \right. \right. \\ \left. \left. - i \langle X, p_s | f_{X'N, XN}^{\text{off}}(s, t) | X', p_{s'} \rangle \tilde{p}_{s', z} \tilde{\Psi}^{SD}(\vec{p}_{s'}, S_i, S_s) \right] \right|^2, \quad (4)$$

where  $\Psi^{SD}$  ( $\tilde{\Psi}^{SD}$ ) is the undistorted (distorted) deuteron wave function with spin projection  $S_D$ ,  $\beta(s, m_{X'}) = \sqrt{(s - (m_n - m_{X'})^2)(s - (m_n + m_{X'})^2)}$  (with  $s$  the Mandelstam variable of the rescattering process),  $m_{X'}$  is the invariant mass of the produced hadronic state before the rescattering and  $\tilde{p}_{s', z} \equiv p_{s, z} - \Delta$ , with

$$\Delta = \frac{v + M_D}{|\vec{q}|} (E_s - m_p) + \frac{m_X^2 - \gamma}{2|\vec{q}|} \quad \text{for } \gamma \leq m_X^2, \\ \Delta = \frac{v + M_D}{|\vec{q}|} (E_s - m_p) \quad \text{for } \gamma > m_X^2, \quad (5)$$

where  $\gamma = m_n^2 + 2m_n v - Q^2$  is the produced DIS mass off the stationary nucleon. The two regimes in Eq. (5) originate from the condition  $m_X^2 > m_{X'}^2$ , which can be inferred from the approximate conservation law for the “-” component in high energy small angle scatterings [11].

The on-shell rescattering amplitude takes the form of Eq. (2). For the off-shell amplitude  $f_{X'N, XN}^{\text{off}}$  there is no clear prescription, but following our main goal of studying the semi-inclusive DIS based only on basic properties of the high-energy scattering we identify two extreme cases for off-shell part of the rescattering amplitude, one when it is taken to be zero (*no off-shell FSI*) and the other in which off-shell amplitude is assumed

to be equal to the on-shell amplitude  $f_{X'N, XN}^{\text{on}}$  referred as *maximal off-shell FSI*. A third approach is to parametrize the amplitude as

$$f_{X'N, XN}^{\text{off}} = f_{X'N, XN}^{\text{on}} e^{-\mu(x, Q^2)t}, \quad (6)$$

with  $\mu$  an extra parameter that can be fitted, providing a measure of the suppression of the off-shell amplitude. This approach is referred to as *fitted off-shell FSI*.

## RESULTS

Fig. 1 compares our model calculations with a selection of data taken in the Deeps experiment (for a definition of the spectral function  $P(p_s, \cos \theta_s)$  see Ref. [1]). For each  $Q^2, W$ , the total cross section  $\sigma$  and slope parameter  $B$  in Eq. (3) were taken as free parameters and fitted to the data for all  $p_s$  values. In the case of the *fitted off-shell FSI*,  $\mu$  was taken as an extra free parameter. As can be observed in the figures, the calculations including FSI do a fair job of describing the data over the kinematic range of the experiment. The differences between the three different off-shell descriptions becomes smaller with higher  $p_s$ . At  $p_s = 300$  MeV the plane-wave and FSI amplitudes are of equal magnitude, making the final result very sensitive to the different descriptions, especially noticeable in the backward region. At this  $p_s$  value, there is also an oscillating structure in the data which disappears with higher  $W$ , but is still present in the model results.

At the higher spectator momenta, the calculations including FSI continuously grow for angles in the forward direction, clearly different from the fairly flat behavior of the plane-wave calculations. This high FSI contribution in the forward region is a consequence of the structure of the phase factor in Eq. (5). At the highest  $p_s$ , the calculations systematically underestimate the data, hinting at a breakdown of the factorization used in the derivation of Eq. (3). Over the whole kinematic range of the data, the *fitted off-shell FSI* calculations are more in agreement with the *no off-shell* than the *maximal off-shell* ones, pointing in the direction of a largely suppressed off-shell rescattering amplitude.

The values of the fitted total cross section  $\sigma$  and slope parameter  $B$  used in Fig. 1 are shown in Figs. 2 and 3 for the *no off-shell FSI* and *maximal off-shell FSI* calculations. After an initial peak at  $W = 1.2$  GeV, corresponding with the creation of a  $\Delta$ , the value of  $\sigma$  drops to around 25 mb and rises with increasing  $W$ . This agrees with the picture of the increased creation of hadronic constituents as  $W$  increases. With increasing  $Q^2$ , the value of the  $(XN)$  cross section parameter also becomes consistently smaller in this region, indicating reduced final-state interactions. This could point at the onset of a color transparency signal, but more data points at other  $Q^2$  and  $W$  values are needed to make more substantial claims. The value of the slope parameter  $B$  is also largely correlated with the  $Q^2, W$ -dependence of the  $\sigma$  parameter.

## NEUTRON STRUCTURE AT HIGH $x$

We now use the Deeps data and our model calculations to outline a method to extract the neutron structure function  $F_2$  at high  $x$  from kinematics at low  $x$ . It is based on

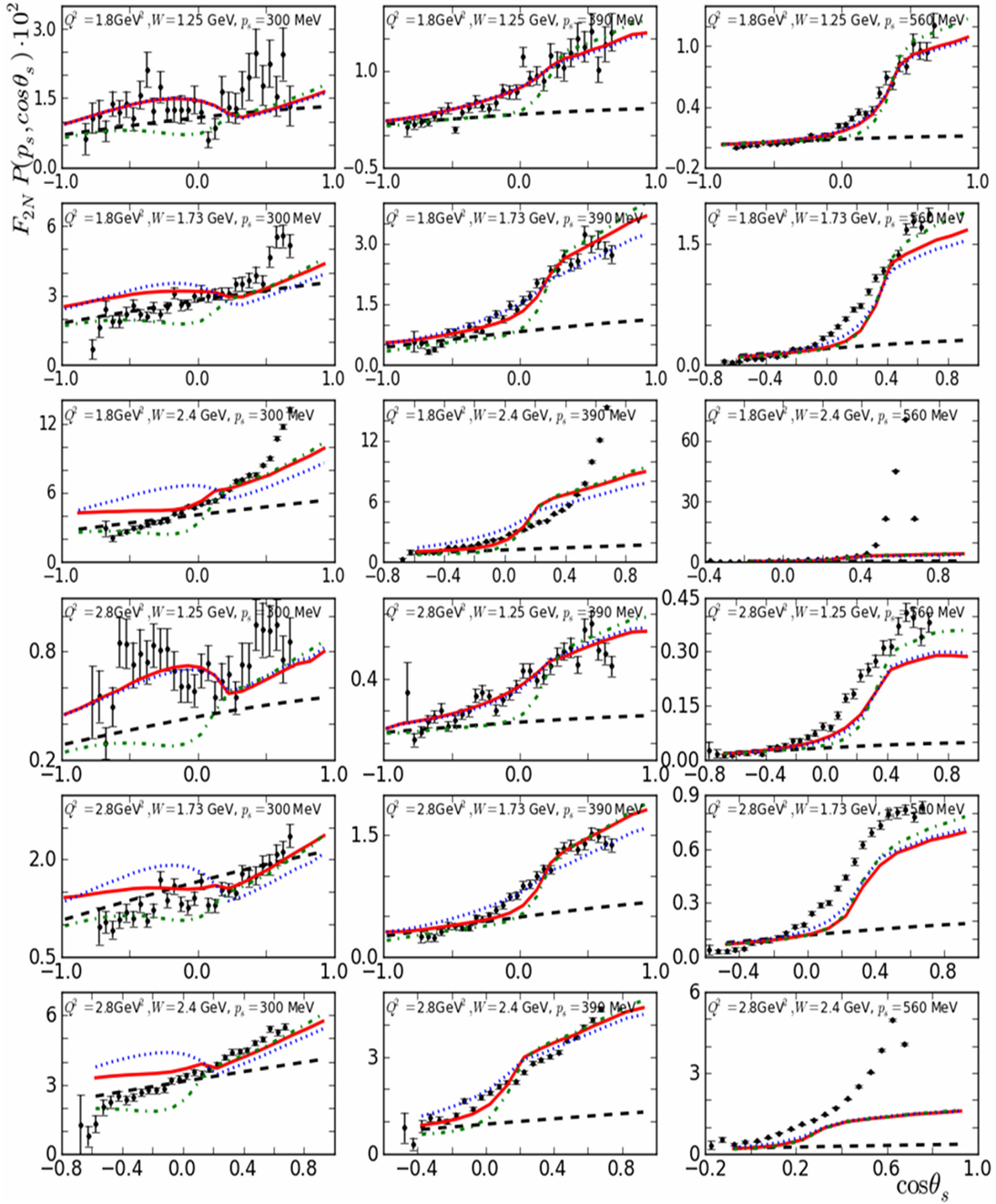


**FIGURE 1.** (Color online) Comparison between the Deeps data [1] and model calculations. The dashed black curve is a plane-wave calculation, the other include final-state interactions. The effective total cross section  $Q^2$  and slope parameter in the final-state interaction amplitude are fitted parameters for each  $Q^2, W$ , the real part is fixed at  $\varepsilon = -0.5$ . The dot-dashed green curve only considers on-shell rescattering, the dotted blue curve has an off-shell rescattering amplitude equal to the on-shell one and the full red curve uses the off-shell parameterization of Eq. (6)

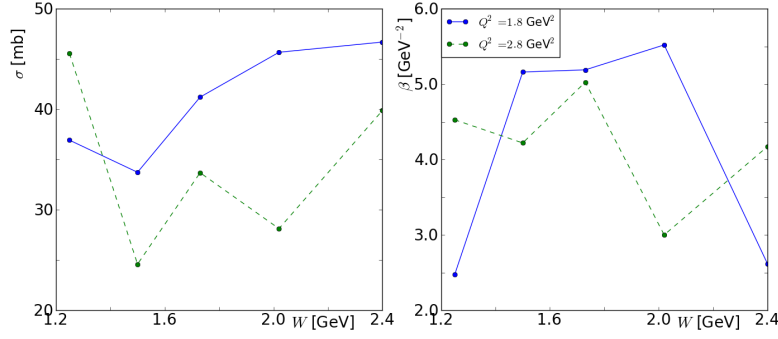


**FIGURE 2.** (Color online) The fitted values of effective cross section  $\sigma$  and slope factor  $B$  for the *no off-shell FSI* calculations used in Fig. 1 as a function of the invariant mass  $W$ . Full blue curve is for  $Q^2 = 1.8 \text{ GeV}^2$ , the dashed green curve for  $Q^2 = 2.8 \text{ GeV}^2$ .

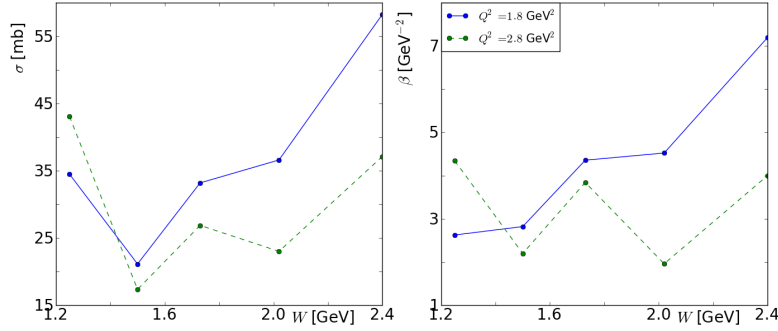


**FIGURE 3.** (Color online) The fitted values of effective cross section  $\sigma$  and slope factor  $B$  for the *maximal off-shell FSI* calculations used in Fig. 1 as a function of the invariant mass  $W$ . Full blue curve is for  $Q^2 = 1.8 \text{ GeV}^2$ , the dashed green curve for  $Q^2 = 2.8 \text{ GeV}^2$ .

an analytical continuation of the amplitude to the unphysical limit  $t' = m_n^2 - p_i^2 \rightarrow 0$ , which corresponds to an on-shell neutron. Due to the low binding energy of the deuteron this singularity of the amplitude is very close to the physical region. It is analogous to the Chow-Low procedure applied in the extraction of  $\pi\pi$  and  $NN$  cross sections from  $p(\pi, p)X$  and  $d(n, n)pn$  reactions [22]. It can be shown that the plane-wave part of the distorted spectral function in Eq. (4) has a double pole in  $t'$ , while the FSI part hasn't [5]. This allows us to extract the  $F_2$  structure function as

$$\lim_{t' \rightarrow 0} F_{2N}^{\text{extr}}(Q^2, \hat{x}, t') = \frac{t'^2}{[\text{Res}(\Psi_D(t' = 0))]^2} \frac{F_L^{D, \text{exp}}(x, Q^2) + v_T F_T^{D, \text{exp}}(x, Q^2)}{\frac{2\hat{x}v}{m_n} \left[ \left( \frac{\alpha_i}{\alpha_q} + \frac{1}{2\hat{x}} \right)^2 + \frac{p_T^2}{2Q^2} \left( \frac{Q^2}{|q|^2} + \frac{2 \tan^2 \frac{\theta_e}{2}}{1+R} \right) \right]}, \quad (7)$$

where  $F_{L,T}^{D, \text{exp}}$  are the experimentally measured deuteron structure functions. The rhs of Eq. (7) has a quadratic dependence on  $t'$ .

The approach we now take is to take a trajectory through the Deeps data at a fixed angle that starts at high  $W, p_s$  and goes to low  $W, p_s$  values. This translates into a descending series in  $t' \rightarrow 0$  and an ascending series in  $\hat{x} \rightarrow x$ , as is shown in Fig. 4.

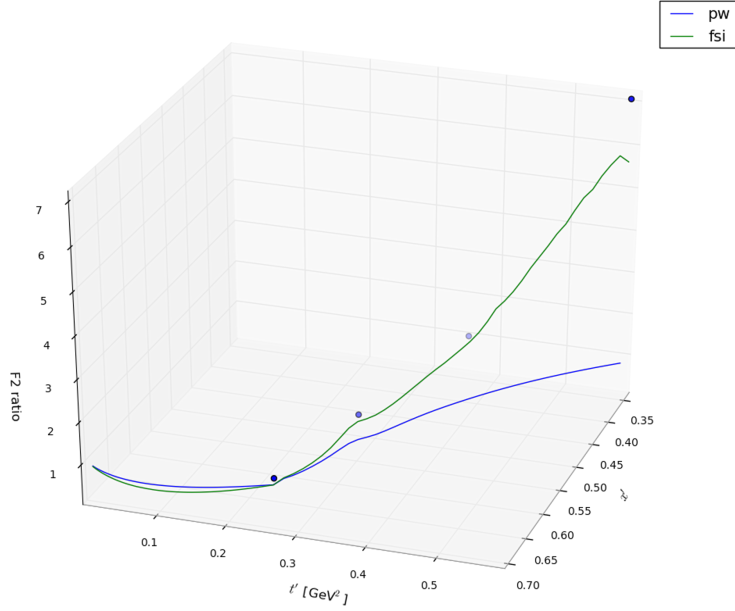


**FIGURE 4.** (Color online) Example of a trajectory in  $t', \hat{x}$  used in the extrapolation procedure for the neutron structure function  $F_2$ . The z-axis shows the ratio of Eq. (7) to the parametrization of Ref. [21]. The blue (green) curve shows the plane-wave (FSI) model calculations along the trajectory, blue dots are JLab Deeps data [1].

In this manner, we can use measurements at low values of  $\hat{x}$  - where  $F_{2N}$  is well known - to extrapolate to regions with high  $x$ .

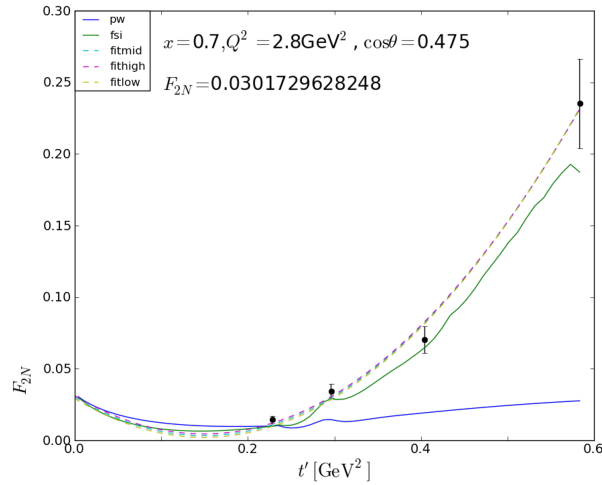


**FIGURE 5.** (Color online) Example of an extrapolation for  $F_{2N}$  at  $x = 0.7$ . The blue (green) curve shows the plane-wave (FSI) model calculations along the trajectory, black dots are JLab Deeps data [1]. The dashed curves are a quadratic fit to the data points, the intercept at  $t' = 0$  yields the  $F_{2N}(x = 0.7)$  value.

Fig. 5 shows an example of a quadratic fit to the Deeps data, extrapolated to  $t' = 0$  to

obtain the neutron structure function  $F_{2N}$  at Bjorken  $x = 0.7$ . As the available data sits on one arm of the quadratic curve, it's not straightforward to do the extrapolation. Here, we imposed an extra constraint on the quadratic fit, that the  $t'$  value of its minimum has to coincide with the minimum of the FSI curve along the trajectory. The position of this minimum is related to the size of the FSI term in the distorted spectral function which the model does a good of describing for the kinematics along this trajectory. The three different fit curves were obtained by taking the data point and error bar values respectively for the lowest  $t'$  data point. With the current data set, the method doesn't provide a robust prediction for the high  $x$  neutron structure function, as trajectories with different spectator angles yield a range of values for  $F_{2N}$ . Ideally, more data at lower  $p_s$  values would provide better constraints and yield better predictions.

## ACKNOWLEDGMENTS

This work is supported by the Research Foundation Flanders as well as by the U.S. Department of Energy Grant under Contract DE-FG02-01ER41172.

## REFERENCES

1. A. V. Klimenko, et al., *Phys. Rev.* **C73**, 035212 (2006), nucl-ex/0510032.
2. H. Fenker, C. Keppel, S. Kuhn, and W. Melnitchouk (2003), URL [http://jlab.org/exp\\_prog/CEBAF\\_EXP/E03012.html](http://jlab.org/exp_prog/CEBAF_EXP/E03012.html), JLAB-PR-03-012.
3. S. Simula, *Phys. Lett.* **B387**, 245–252 (1996), nucl-th/9605024.
4. W. Melnitchouk, M. Sargsian, and M. I. Strikman, *Z. Phys.* **A359**, 99–109 (1997), nucl-th/9609048.
5. M. Sargsian, and M. Strikman, *Phys. Lett.* **B639**, 223–231 (2006), hep-ph/0511054.
6. C. Ciofi degli Atti, L. P. Kaptari, and S. Scopetta, *Eur. Phys. J.* **A5**, 191–207 (1999), hep-ph/9904486.
7. C. Ciofi degli Atti, and B. Z. Kopeliovich, *Eur. Phys. J.* **A17**, 133–144 (2003), nucl-th/0207001.
8. C. Ciofi degli Atti, L. P. Kaptari, and B. Z. Kopeliovich, *Eur. Phys. J.* **A19**, 145–151 (2004), nucl-th/0307052.
9. V. Palli, C. Ciofi degli Atti, L. P. Kaptari, C. B. Mezzetti, and M. Alvioli, *Phys. Rev.* **C80**, 054610 (2009), 0911.1377.
10. C. C. d. Atti, and L. P. Kaptari (2010), 1011.5960.
11. W. Cosyn, and M. Sargsian (2010), 1012.0293.
12. M. M. Sargsian, S. Simula, and M. I. Strikman, *Phys. Rev.* **C66**, 024001 (2002), nucl-th/0105052.
13. M. M. Sargsian, *Phys. Rev.* **C82**, 014612 (2010), 0910.2016.
14. M. M. Sargsian, *Int. J. Mod. Phys.* **E10**, 405–458 (2001), nucl-th/0110053.
15. M. M. Sargsian, et al., *J. Phys.* **G29**, R1 (2003), nucl-th/0210025.
16. L. L. Frankfurt, and M. I. Strikman, *Physics Reports* **76**, 215 – 347 (1981).
17. L. L. Frankfurt, and M. I. Strikman, *Phys. Lett.* **B64**, 433–434 (1976).
18. L. L. Frankfurt, and M. I. Strikman, *Physics Letters B* **183**, 254 – 258 (1987).
19. P. V. Landshoff, and J. C. Polkinghorne, *Phys. Rev.* **D18**, 153 (1978).
20. S. Jeschonnek, *Phys. Rev.* **C63**, 034609 (2001), nucl-th/0009086.
21. A. Bodek, M. Breidenbach, D. L. Dubin, J. E. Elias, J. I. Friedman, H. W. Kendall, J. S. Poucher, E. M. Riordan, M. R. Sogard, D. H. Coward, and D. J. Sherden, *Phys. Rev. D* **20**, 1471–1552 (1979).
22. G. F. Chew, and F. E. Low, *Phys. Rev.* **113**, 1640–1648 (1959).